Electronic Supplementary Information

Pyridinic nitrogen-rich carbon nanocapsules from a bioinspired polydopamine derivative for highly efficient electrocatalytic oxygen reduction

Zhengran Yi,[a§] *Zheye Zhang,*[a§] *Shuai Wang,**[a] *and Gaoquan Shi**[b]

[a]School of Chemistry and Chemical Engineering, Huazhong University of Science and Technology, Wuhan 430074, PR China.

*E-mail: chmsamuel@mail.hust.edu.cn

[b]Department of Chemistry, Tsinghua University, Beijing 100084, PR China.

*E-mail: gshi@tsinghua.edu.cn

[§]These authors contributed equally to this work.

1. Experimental Section

Synthesis of 2-Bromo-6-iodo-3-[(4-methoxyphenyl)methoxy]pyridine (compound 2): 2-Bromo-3-hydroxy-6-iodopyridine (compound 1) was synthesized according to the literature.[S1] Compound 1 (60 g, 200.07 mmol) was dissolved in DMF (700 mL), and then K_2CO_3 (55.3 g, 400.14 mmol) and 1-(chloromethyl)-4-methoxybenzene (34.5 g, 220.08 mmol) were added. This mixture was stirred at 90 °C for 18 h, and followed by the addition of H_2O to quench the reaction. A solid formed during the process and was collected by filtration and dried in vacuo to afford a light brown solid (45 g, 99.7 %). ^{1}H NMR (400 MHz, $CDCl_3$, δ ppm): 7.54 (d, 1H), 7.35 (d, 2H), 6.93 (d, 2H), 6.86 (d, 1H), 5.09 (s, 2H), 3.82 (s, 3H). ^{13}C NMR (100 MHz, $CDCl_3$, δ): 159.79, 152.52, 134.08, 129.42, 128.89, 127.01, 122.67, 114.22, 101.82, 71.16, 55.32. HRMS (ESI) m/z: $[M]^+$ Calcd. for $C_{13}H_{11}BrINO_2$ 418.90; Found 418.38.

Synthesis of 6-Iodo-2-methoxy-3-[(4-methoxyphenyl)methoxy]pyridine (compound 3): To a solution of compound 2 (45 g, 200.07 mmol) in DMF (500 mL) was added CH_3ONa (8.7 g, 160.70 mmol). The mixture was stirred at 100 °C for 2 h, and followed by the addition of H_2O to quench the reaction. The crude product was filtered off and subsequently purified by column chromatography on silica gel to afford a white solid (32 g, 80 %). ^{1}H NMR (400 MHz, $CDCl_3$, δ ppm): 7.32 (d, 2H), 7.16 (d, 1H), 6.91 (d, 2H), 6.74 (d, 1H), 5.03 (s, 2H), 3.95 (s, 3H), 3.81 (s, 3H). ^{13}C NMR (100 MHz, $CDCl_3$, δ): 159.66, 154.55, 143.22, 129.15, 127.89, 127.17, 122.28, 114.12, 100.19, 70.85, 55.31, 53.87. HRMS (ESI) m/z: $[M+Na]^+$ Calcd. for $C_{14}H_{14}INNaO_3$ 393.99; Found 393.99.

Synthesis of 6-methoxy-5-[(4-methoxyphenyl)methoxy]-2-pyridineacetonitrile (compound 4): To a solution of compound 3 (32 g, 86.21 mmol) in DMF (500 mL) were added $Pd_2(dba)_3$ (1.6 g, 1.72 mmol), $P(t\text{-}Bu)_3$ (880 mg, 4.31 mmol), trimethylsilyl acetonitrile (19.5 g, 172.43 mmol) and zinc fluoride (8.9 g, 86.21 mmol). This mixture was stirred at 150 °C for 7 h. After cooling to ambient temperature, the reaction solution was poured into H_2O and extracted with ethyl acetate. The combined organic phase was dried over $MgSO_4$, filtered, concentrated, and finally purified by column chromatography on silica gel to afford a yellow solid (21 g, 86 %). ^{1}H NMR (400 MHz, $CDCl_3$, δ ppm): 7.34 (d, 2H), 7.03 (d, 1H), 6.91 (d, 2H), 6.84 (d, 1H), 5.07 (s, 2H), 4.00 (s, 3H), 3.81 (s, 3H), 3.74 (s, 2H). ^{13}C NMR (100 MHz, CDCl3, δ): 159.63, 142.60, 137.80, 129.14, 128.06, 120.37, 117.49, 114.76, 114.11, 70.74, 55.31, 53.87, 25.42. HRMS (ESI) m/z: $[M]^+$ Calcd. for $C_{16}H_{16}N_2O_3$ 284.12; Found 284.22.

Synthesis of 6-methoxy-5-[(4-methoxyphenyl)methoxy]-2-pyridine ethanamine (compound 5): To a solution of compound 4 (21 g, 73.86 mmol) in MeOH (200 mL) was added Raney Ni (1.0 g, 7.39 mmol) and concentrated HCl (60 mL, 738.6 mmol) and the system was stirred under an atmosphere of hydrogen via a balloon for 2 h. The reaction products were filtered through a pad of celite and washed through with MeOH. The filtrate was basified to a pH value of 9 using saturated aqueous sodium carbonate. Methanol was removed under vacuo and the resulting residue was partitioned with water and a mixture of chloroform and ethanol (4:1). The organic phase was dried over $MgSO_4$, filtered, concentrated to afford a white solid (21 g, 86 %). ^{1}H NMR (400 MHz, $CDCl_3$, δ ppm): 7.24 (d, 2H), 7.03 (d, 1H), 6.81 (d, 2H), 6.58 (d, 1H), 4.78 (s, 2H), 3.84

(s, 3H), 3.67 (s, 3H), 3.28 (m, 2H), 2.66 (m, 2H). ^{13}C NMR (100 MHz, CDCl3, δ): 159.67, 154.30, 147.41, 141.25, 129.13, 128.76, 121.18, 115.36, 113.46, 70.44, 54.29, 52.23, 39.94, 36.25. HRMS (ESI) m/z: HRMS (ESI) m/z: $[M+Na]^+$ Calcd. for $C_{14}H_{14}INNaO_3$ 311.15; Found 311.13.

Synthesis of 6-(2-aminoethyl)-3-hydroxy-pyridin-2(1H)-one (AHPO) hydrobromide (compound 6): Compound 5 was added to a solution of hydrobromic acid (40 %) in acetic acid at room temparature, the suspension was then heated to 80 °C, and stirred for 12 h, the acid was removed under vacuum to give a crude product. The crude product was stirred with DCM (50 mL) for 2 h, filtered and washed with DCM (30 mL), and dried to afford a light green solid (13 g, 76 %). ^{1}H NMR (400 MHz, $CDCl_3$, δ ppm): 7.35 (dd, 1H), 6.81 (dd, 1H), 3.31 (m, 2H), 3.10 (m, 2H). ^{13}C NMR (100 MHz, $CDCl_3$, δ): 155.62, 143.43, 134.92, 125.53, 114.87, 38.42, 29.40. HRMS (ESI) m/z: [M]+ Calcd. for $C_7H_{11}N_2O_2$ 115.08; Found 115.07.

Poly-AHPO (PAHPO) coating: AHPO hydrobromide (3 mg/mL) was dissolved in 15 mM Tris under stirring, and substrates containing metal nickel foil, polyurethane sponge and silica nanospheres were dipped into the solution. pH-induced oxidation changes the solution color from yellow to black.

Preparation of PAHPO-derived N-doped carbon nanocapsules (PAP-NCNCs): Silica nanospheres were synthesized as templates by Stöber method.[S2] First, silica nanospheres (500 mg) were mixed with the synthesized AHPO hydrobromide (150 mg) in Tris-buffer (50 mL, 15 mM) for 60 h. The poly-AHPO (PAHPO)/silica nanocomposite obtained was collected by centrifugation, then carbonized under N_2

atmosphere at 900 ^{o}C for 1 h with a heating rate of 10 ^{o}C min^{-1}. After washing in 5 M NaOH aqueous solution for 4 h and subsequent freeze-drying, PAP-derived NCNCs were finally obtained. Polydopamine-derived NCNCs (PDA-NCNCs) were prepared under a similar procedure with dopamine as precursor.

Characterizations: The structures and morphology of the samples were characterized by NMR spectra (Bruker AVANCE III-400 spectrometer), mass spectra (Ion Spec 4.7 T FTMS instrument), field-emission scanning electron microscope (SEM, FEI, Nova NanoSEM 450) and field-emission transmission electron microscope (TEM, FEI, Tecnai G2 F30). The electron energy loss spectroscopy (EELS) spectra and mappings were performed on the field-emission TEM. X-ray photoelectron spectroscopy (XPS) measurements were taken on a VG ESCALAB 250 spectrometer with an Al Kα X-ray source (1486 eV), X-ray radiation (15 kV and 10 mA), and hemispherical electron energy analyzer. Raman spectra were recorded on a confocal laser micro-Raman spectrometer (Thermo Fischer DXR, USA) equipped with a He-Ne laser of excitation of 532 nm.

Electrocatalytic performance measurements: All of the electrochemical measurements were performed in a conventional three-electrode cell using a rotating ring disk electrode rotator (RRDE-3A, Japan) and a CHI 760E electrochemical analyzer (CH Instruments, Inc., Shanghai). Hg/HgO (0.1 M NaOH) electrode and platinum mesh were used as reference and counter electrodes, respectively. All potentials measured were calibrated to reversible hydrogen electrode (RHE) using the following equation: $E(RHE) = E(Hg/HgO) + 0.165\ V + 0.0591 \times pH$. A rotating disk electrode (RDE) with

a glassy carbon disk (5 mm diameter) and a rotating ring-disk electrode (RRDE) electrode with a Pt ring (5 mm inner diameter and 7 mm outer diameter) served as the substrate for the working electrodes for evaluating the oxygen reduction reaction (ORR) activities. To prepare the working electrodes, 5 mg catalysts were dispersed in an aqueous solution containing 10 μL Nafion solution (5 wt%) and 1 mL ethanol in an ultrasonic bath. The obtained homogeneous catalyst ink (8 μL) was then dropped onto a mirror-polished glassy carbon electrode. A 0.1 M KOH aqueous solution saturated with O_2 was used as the electrolyte unless otherwise stated. All linear scan voltammogram (LSV) measurements were conducted at a scan rate of 5 mV s^{-1} at room temperature.

On the basis of RDE data, the kinetic parameters can be analyzed with the Koutecky-Levich equation using the following relationship:

$$1/j_d = 1/j_k + 1/B\omega^{1/2}$$

where j_k is the kinetic current density at a constant potential, j_d is the measured current density, ω is the electrode rotating speed in rpm, and the theoretical value of the Levich slope (B) is evaluated from the following equation:

$$B = 0.2nFv^{-1/6}C_{O2}D_{O2}^{2/3}$$

where n is the overall number of transferred electrons in the ORR process, F is the Faradaic constant (96485 C mol^{-1}), C_{O2} is the bulk concentration (solubility) of O_2 in 0.1 M KOH (1.2×10^{-6} mol cm^{-3}), D_{O2} is the diffusion coefficient of O_2 in 0.1 M KOH (1.9×10^{-5} cm s^{-1}) and v is the kinematic viscosity of 0.1 M KOH (0.01 cm^2 s^{-1}). The constant 0.2 is adopted when the rotating speed is in rpm.

On the basis of RRDE measurements, the electron transfer number (n) and HO_2^- intermediate production percentage ($\%\ HO_2^-$, which serves as $2e^-$ pathway selectivity) were determined as follows:

$$n = \frac{4I_d}{I_d + I_r/N}$$

$$\%\ HO_2^- = \frac{200I_r/N}{I_d + I_r/N}$$

where I_d is the disk current, I_r is the ring current, and $N = 0.37$ is the current collection efficiency of the Pt ring.

Zn–air batteries were tested in home-made electrochemical batteries,[S3] where catalysts loaded on the carbon paper as the air cathode and Zn foil as anode in 6.0 M KOH. Catalyst loading was 0.5 mg cm^{-2} for all materials.

2. Supplementary NMR spectra

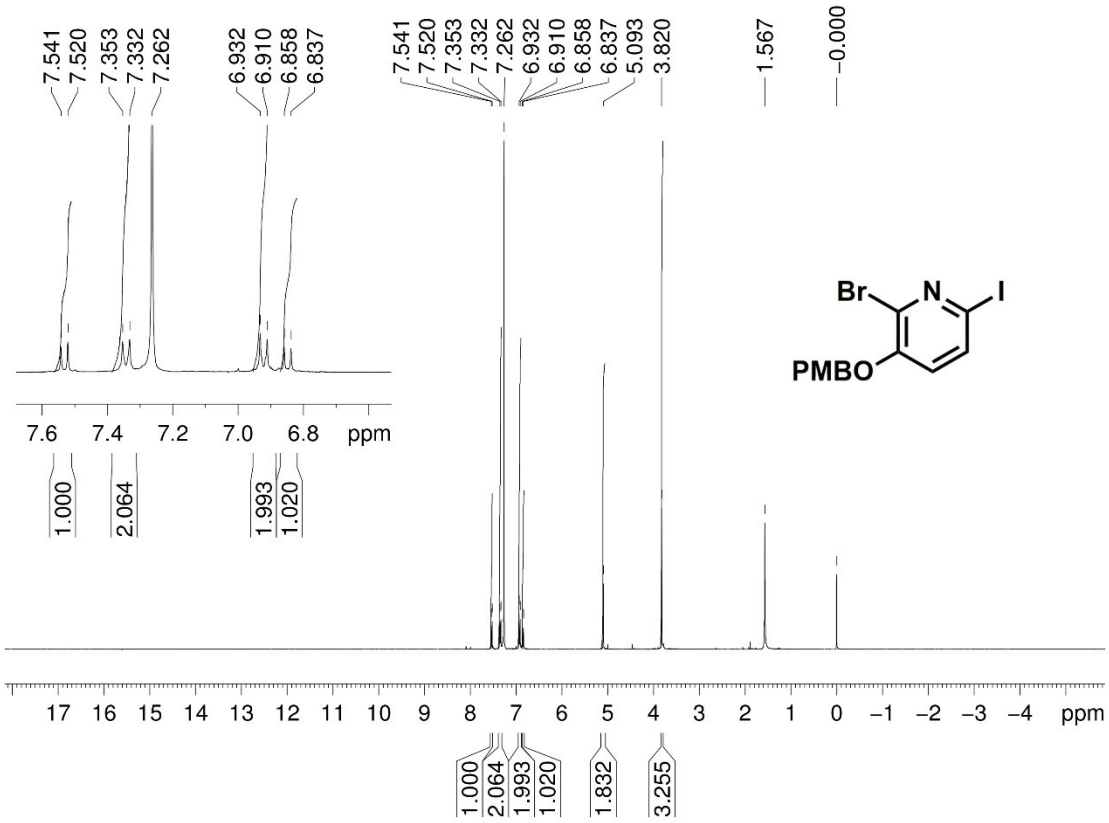

^{1}H NMR spectrum of compound 2 in $CDCl_3$

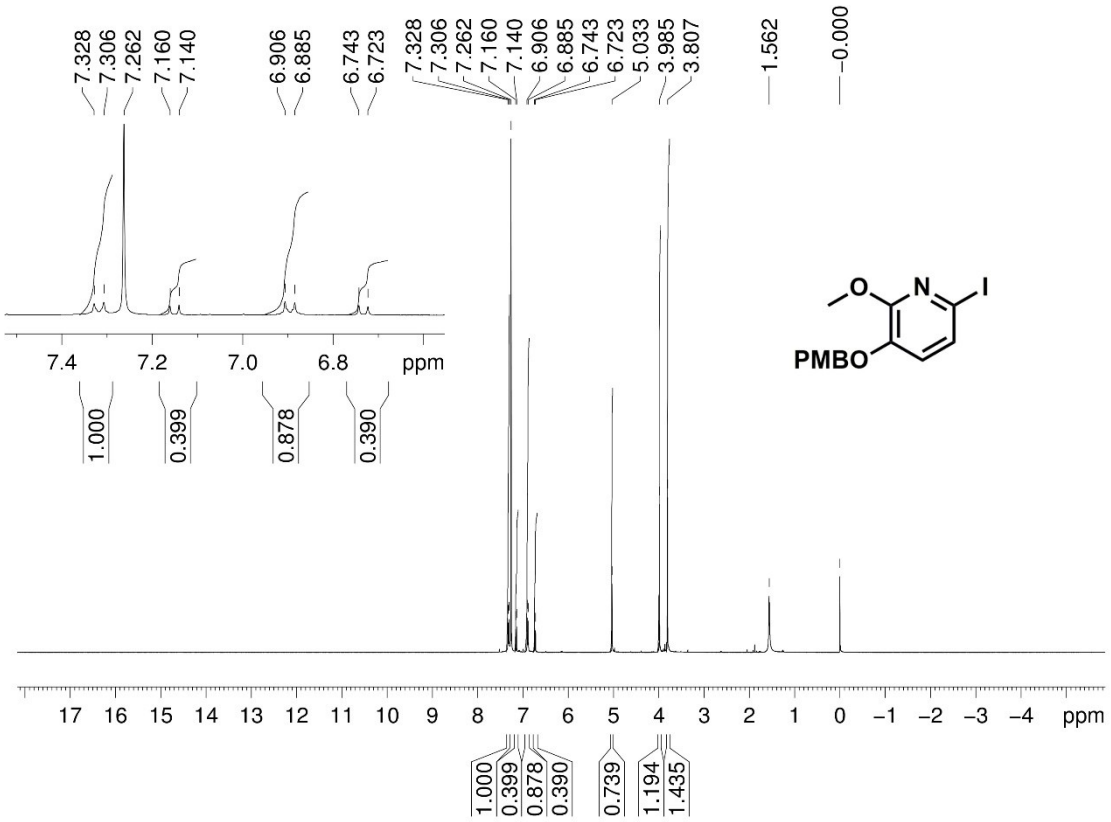

^{1}H NMR spectrum of compound 3 in $CDCl_3$

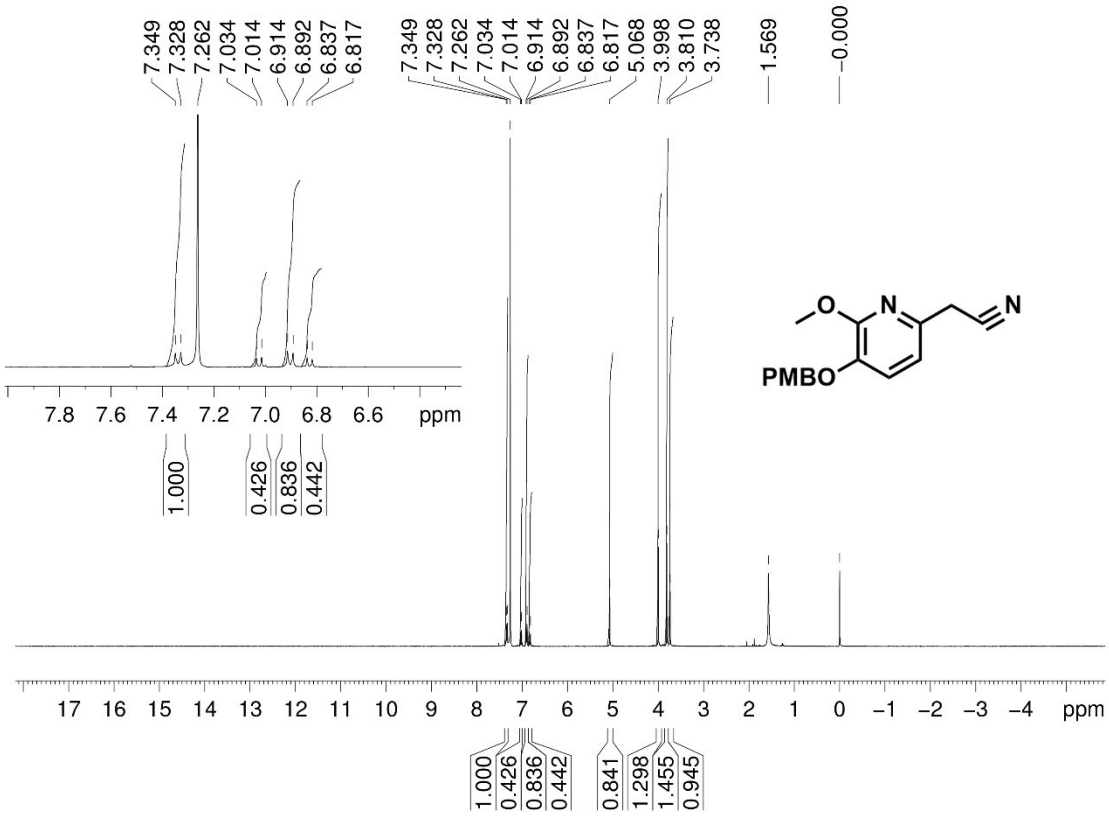

^{1}H NMR spectrum of compound 4 in $CDCl_3$

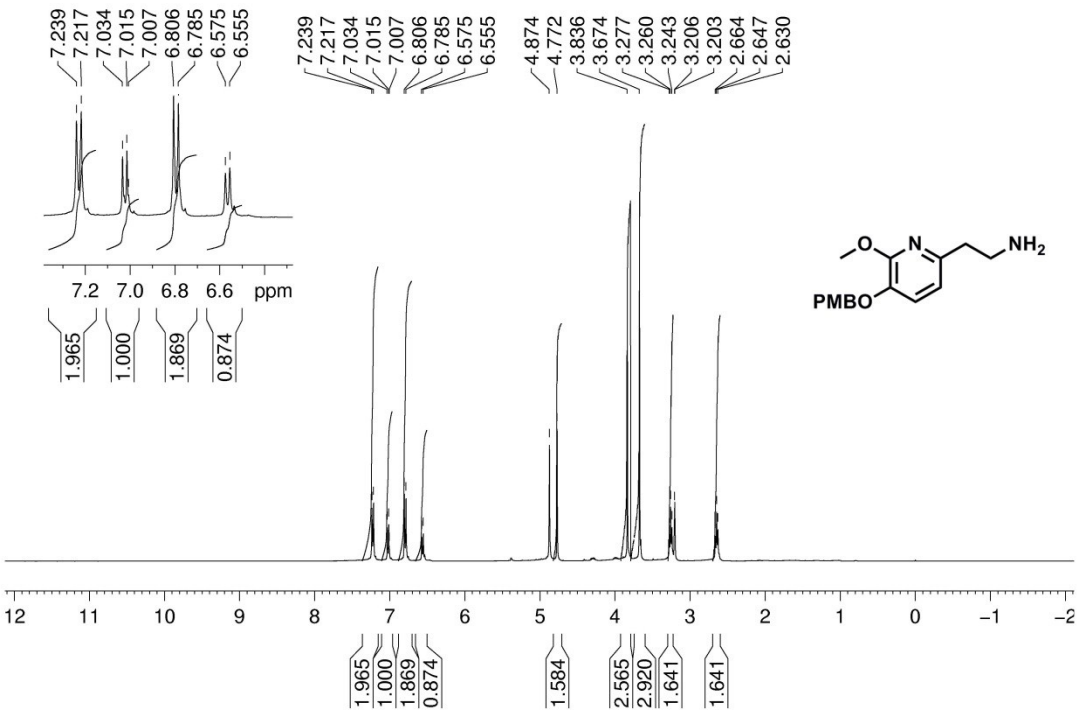

^{1}H NMR spectrum of compound 5 in CD_3OD

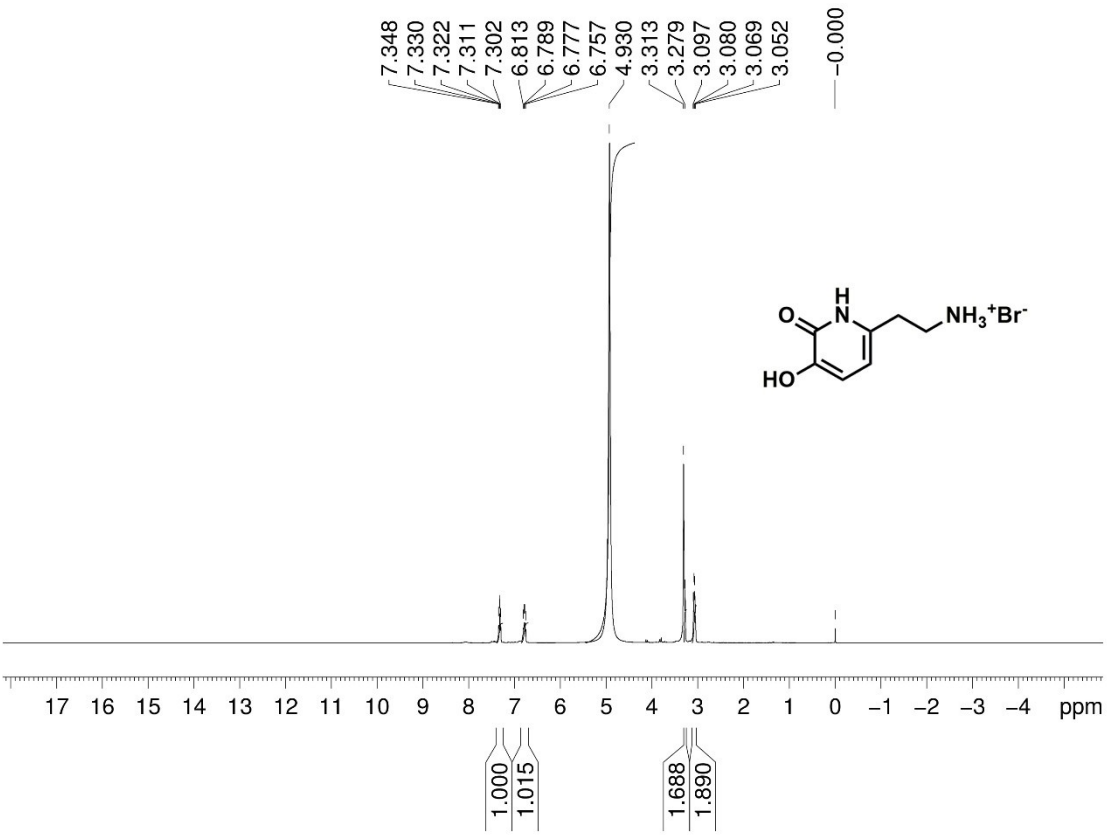

^{1}H NMR spectrum of compound 6 in CD_3OD

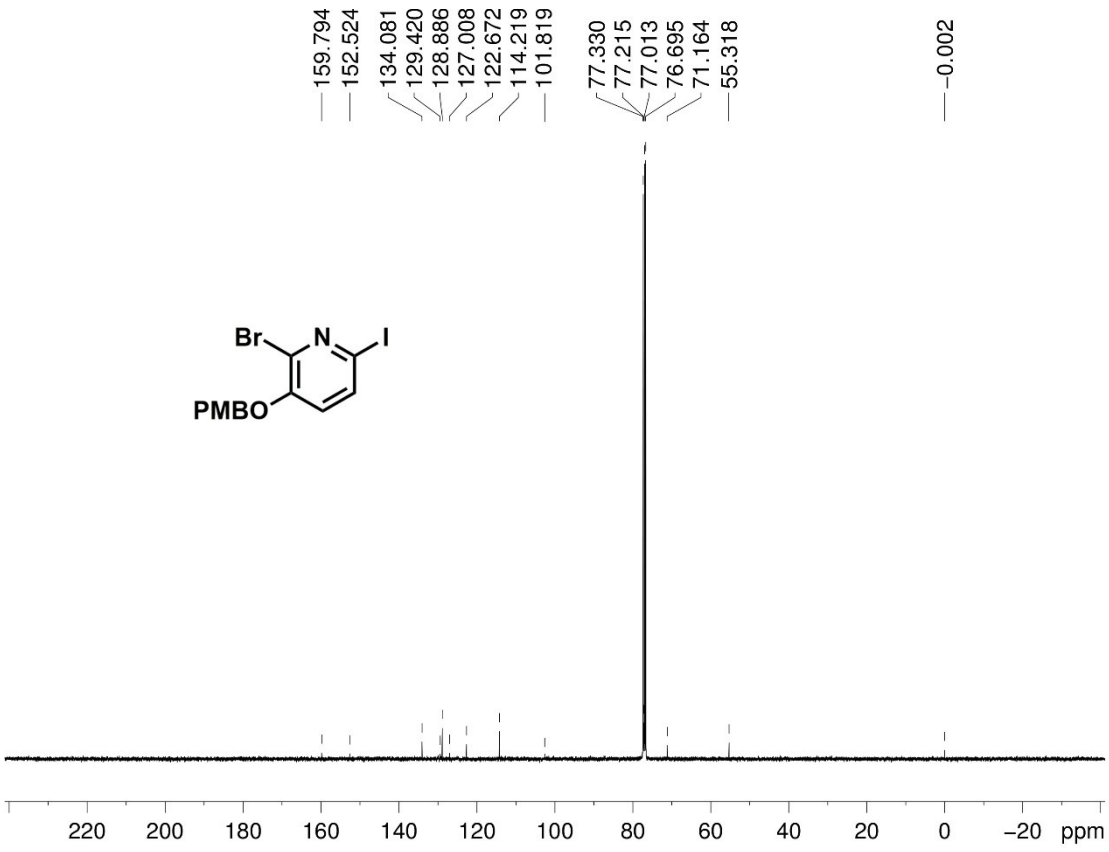

^{13}C NMR spectrum of compound 2 in $CDCl_3$

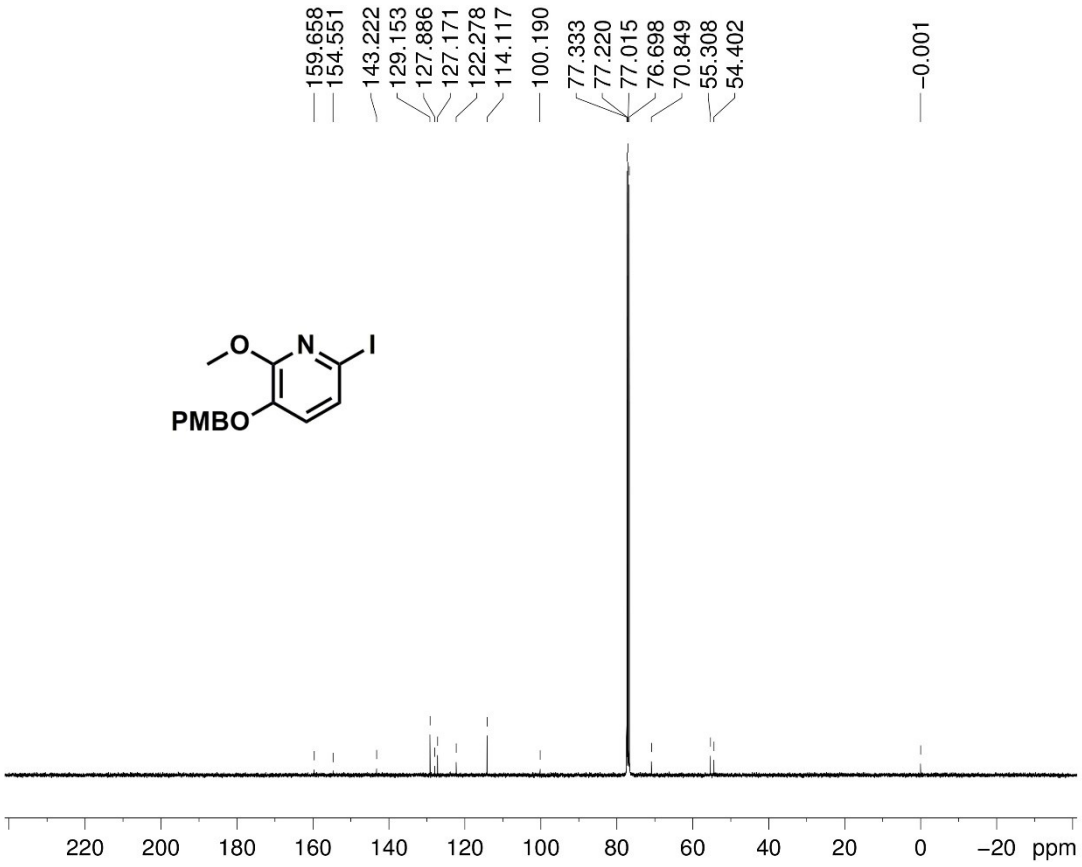

^{13}C NMR spectrum of compound 3 in $CDCl_3$

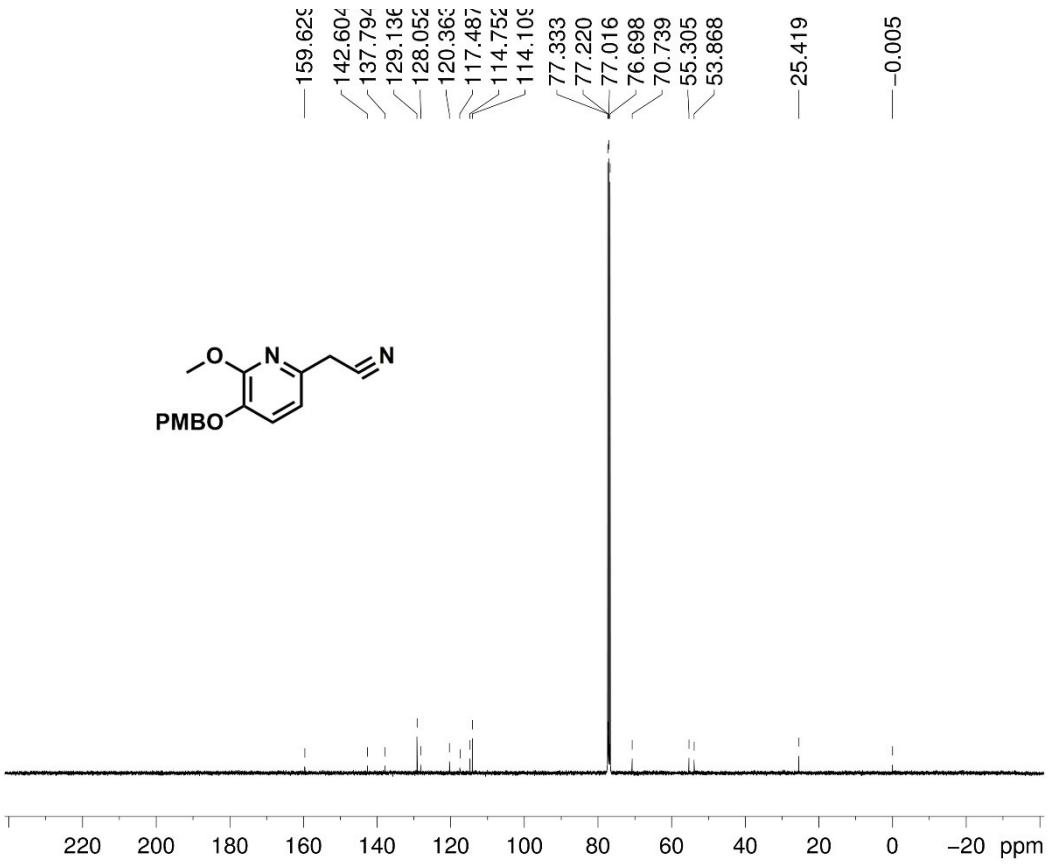

^{13}C NMR spectrum of compound 4 in $CDCl_3$

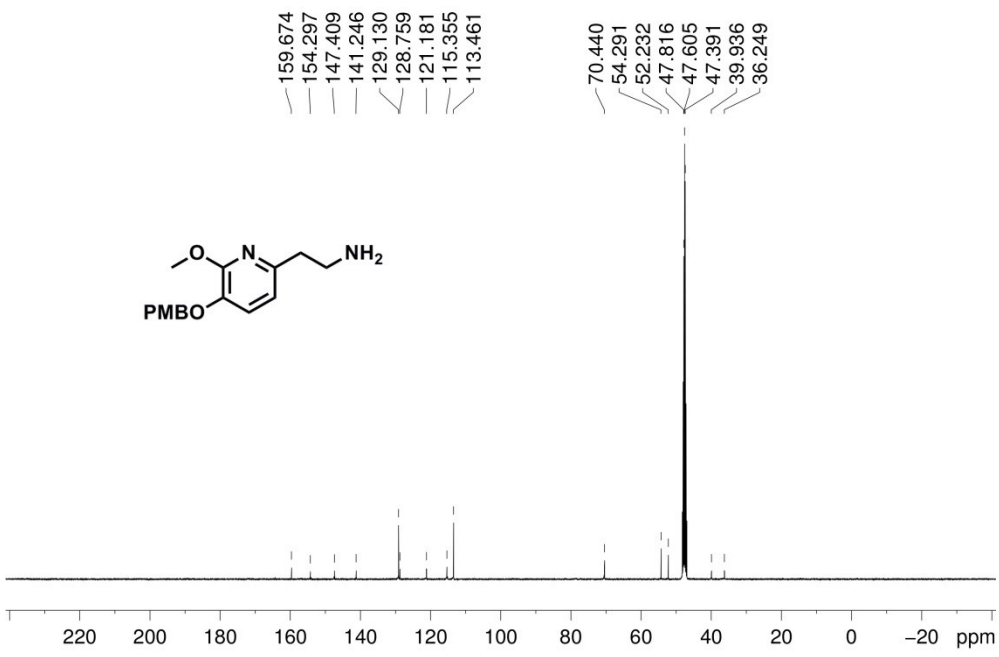

^{13}C NMR spectrum of compound 5 in CD_3OD

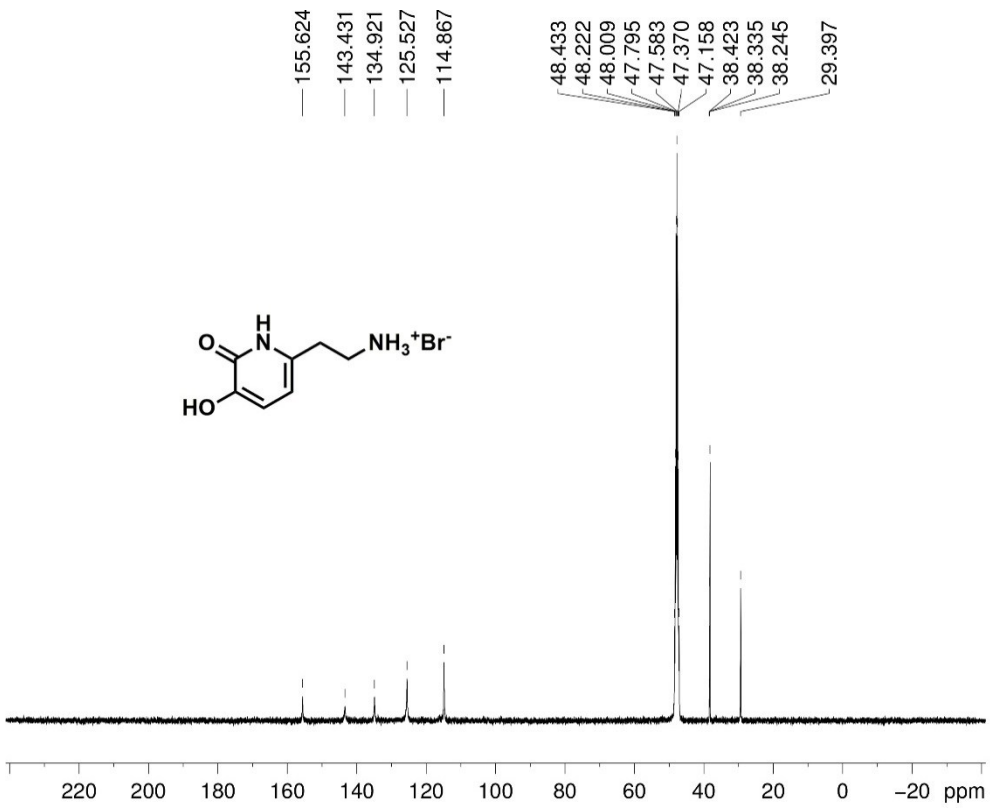

^{13}C NMR spectrum of compound 6 in CD_3OD

3. Supplementary Figures

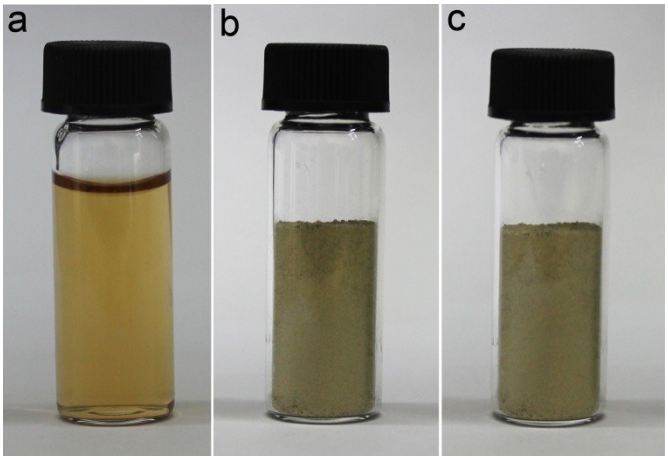

Figure S1. (a) Photograph of the hydrobromide of AHPO solution. (b,c) Photographs of the hydrobromide of AHPO powder (b) before and (c) after keeping in air for three months.

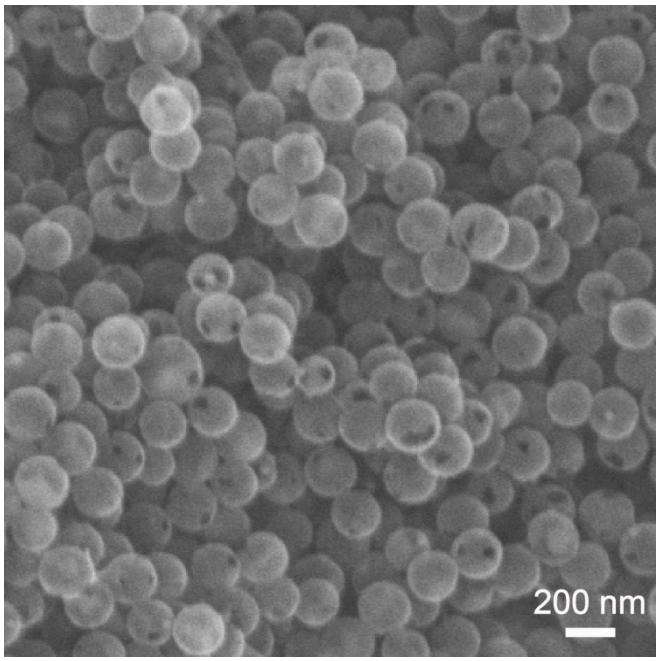

Figure S2. SEM image of PAP-NCNCs.

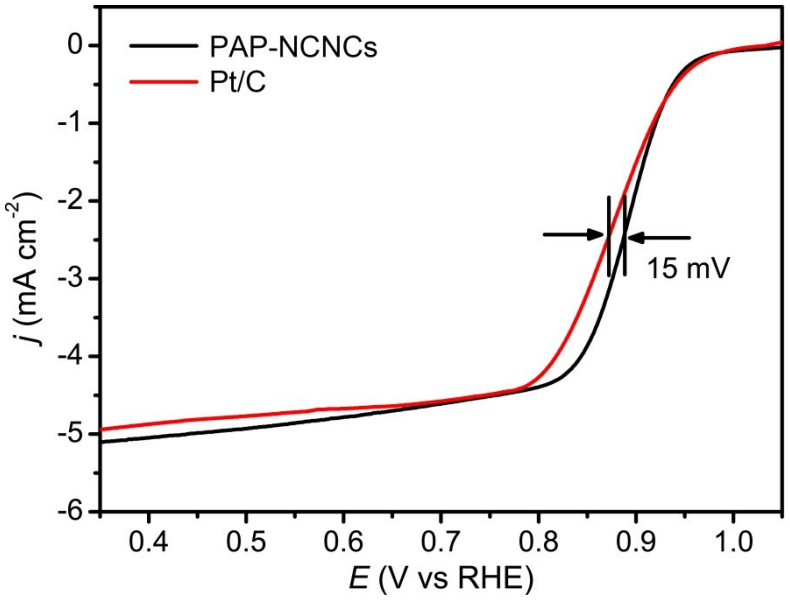

Figure S3. LSV curves of PAP-NCNCs and commercial Pt/C catalyst at 1600 r.p.m. in O_2-saturated 0.1 M KOH solution.

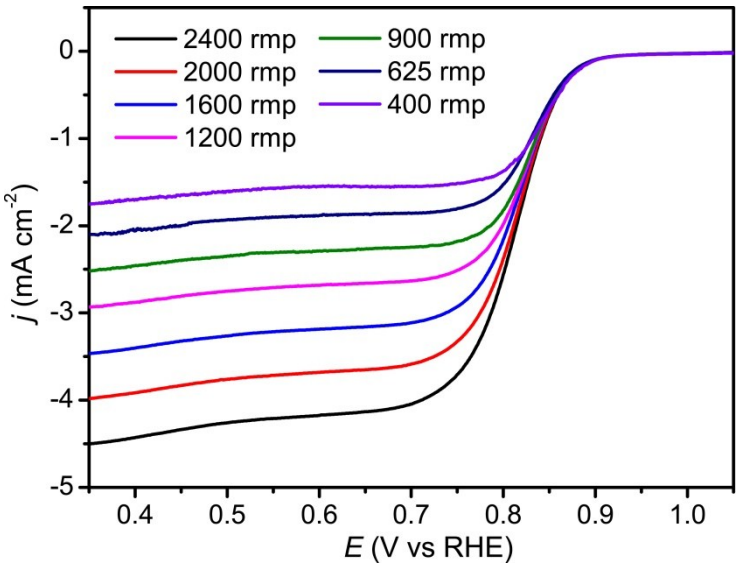

Figure S4. LSV curves of PDA-NCNCs in O_2-saturated 0.1 M KOH with different rotating speeds.

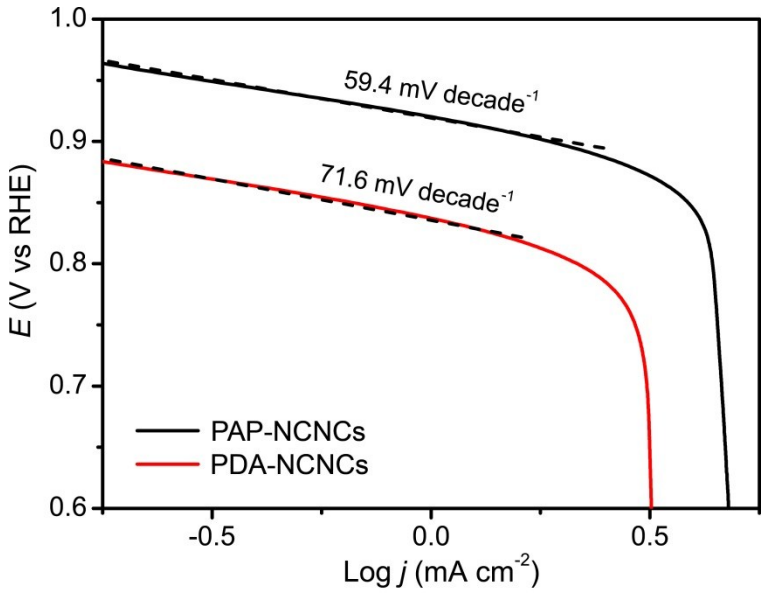

Figure S5. The Tafel plots of PAP-NCNCs and PDA-NCNCs catalysts.

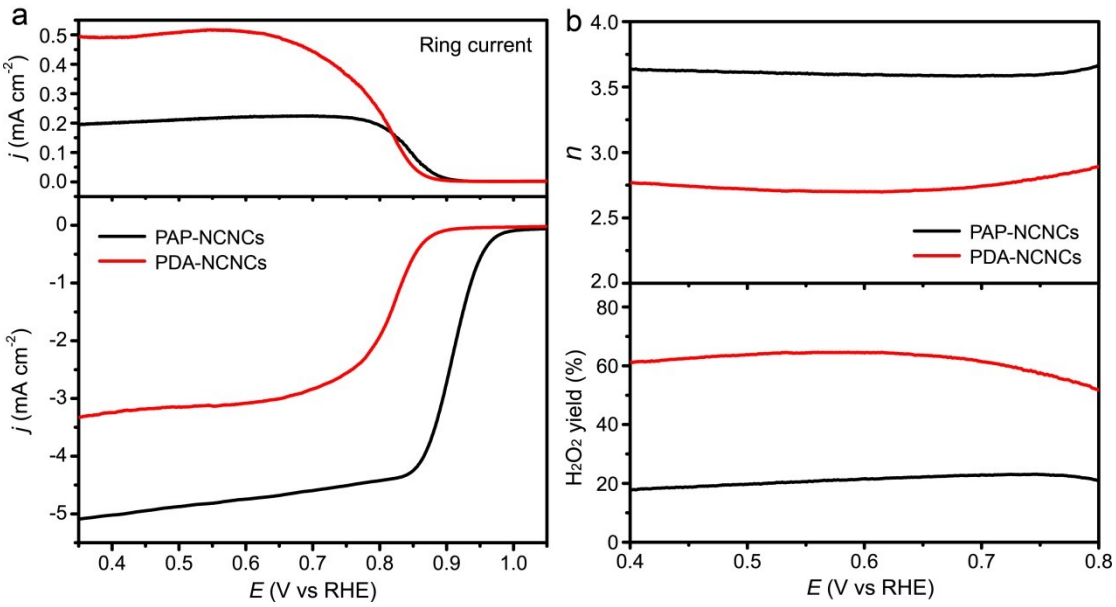

Figure S6. (a) RRDE tests (1600 rpm) of PAP-NCNCs and PDA-NCNCs catalysts for ORR in 0.1 M KOH saturated with O_2. (b) The calculated electron transfer number and H_2O_2 generated from ORR.

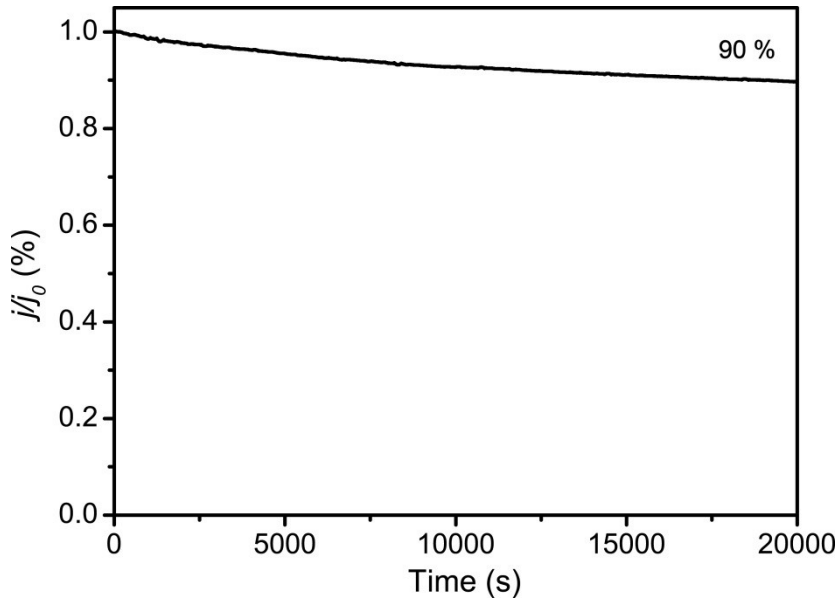

Figure S7. The chronoamperometric response of PDA-NCNCs in O_2-saturated 0.1 M KOH solution at 0.8 V at 1600 rpm.

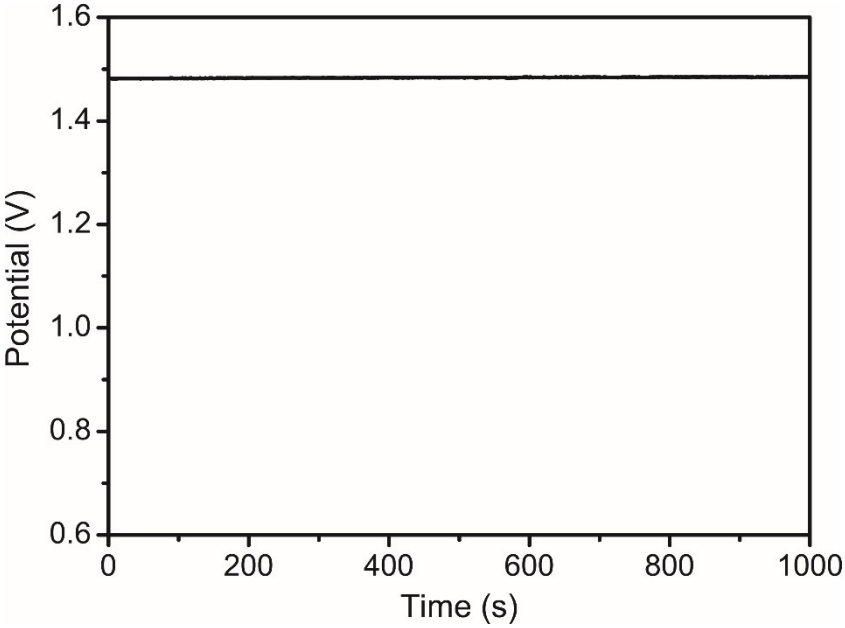

Figure S8. Open circuit voltage measurement of primary Zn–air battery with PAP-NCNCs as the cathode catalyst.

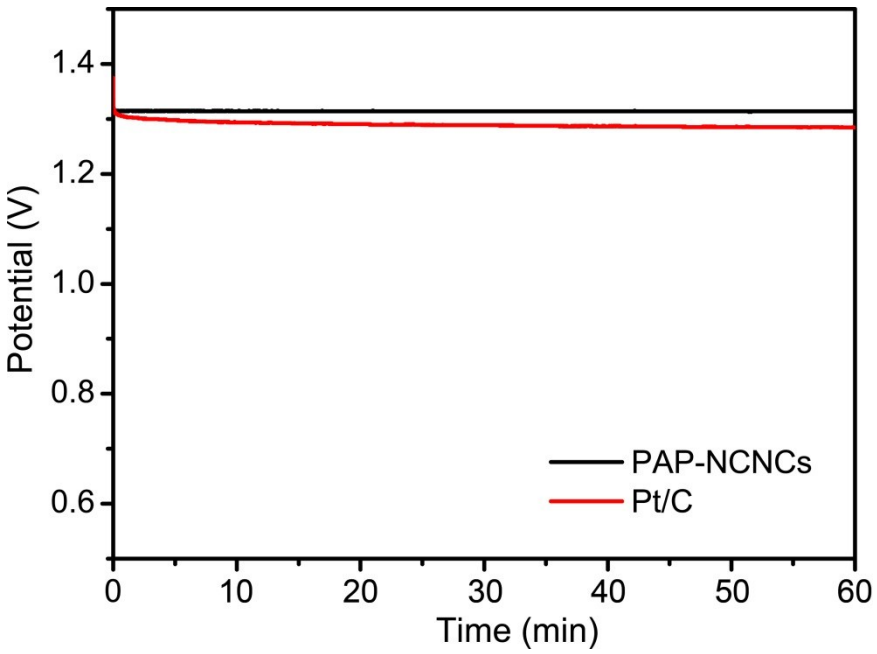

Figure S9. Typical galvanostatic discharge curves of primary Zn–air batteries with PAP-NCNCs and Pt/C as cathode catalysts at a current density of 5 mA cm^{-2}.

4. Supplementary Table

Table S1. ORR parameters of typical comparable samples.

Catalyst	Loading (mg/cm^2)	Onset potential (V)	Current density at 0.8V (mA/cm^2)	Half-wave potential ($E_{1/2}$, V)	Reference
N-doped carbon nanosheets	0.6	0.95	3.2	0.84	Angew. Chem. Int. Ed. 2014, 53, 1570
Mesporous N-doped carbon	0.8	0.93	2.8	0.82	J. Am. Chem. Soc. 2011, 133, 206
N-doped hierarchically porous carbons	0.5	0.98	4.9	0.87	Nat. Commun. 2014, 5, 4973
N-doped mesoporous carbon spheres	0.71	0.90	0.5	0.74	Angew. Chem. Int. Ed. 2015, 54, 588
Carbon nanotubes/ heteroatom-doped carbon	0.6	0.93	3.4	0.81	Angew. Chem. Int. Ed. 2014, 53, 4102
N and P co-doped mesoporous nanocarbon foams	0.5	0.94	3.4	0.85	Nat. Nanotechnol. 2015, 10, 444
N and S co-doped Carbon	unknown	0.91	2.1	0.76	ACS Appl. Mater. Interfaces 2015, 7, 7214
N and B co-doped graphene	0.283	0.87	3.7	0.84	Angew. Chem. Int. Ed. 2013, 52, 3110
N and F dual-doped mesoporous graphene	unknown	0.98	3.6	0.83	Nanoscale 2015, 7, 10584
N-doped ordered macro-mesoporous carbon/graphene	0.42	0.86	0.7	0.73	Adv. Mater. 2013, 25, 6226
Vertically aligned N-doped CNTs	unknown	0.97	2.6	0.84	Science 2009, 323, 760
N-CNF aerogel	0.4	0.97	2.5	0.80	Nano Energy 2015, 11, 366
Pt/C (20 %)	**0.2**	**0.99**	**4.3**	**0.872**	**This work**
PAP-NCNCs	**0.2**	**0.98**	**4.4**	**0.887**	**This work**

Note: The N contents for all samples in this table range from 2.0 at. % to 9.4 at. %.

Table S2. The performance of primary Zn-air batteries with various electrocatalysts.

Catalyst	Loading (mg cm^{-2})	Peak power density (mA cm^{-2})	Specific capacity (mAh g_{Zn}^{-1})	Reference
Porous N doped graphene	-	70	400	J. Mater. Chem. 2012, 22, 12810
CoO/N-CNT	1.0	265	570	Nat. Commun. 2013, 4, 1805
N doped graphene	0.7	42	-	J. Electrochem. Soc. 2013, 160, F910.
MnO_2/Co_3O_4	2.0	36	-	Nanoscale 2013, 5, 4657
N-doped hierarchically porous carbons	1.0	-	630	Nat. Commun. 2014, 5, 4973
Nitrogen-doped carbon nanofiber	1.0	-	615	Nano Energy 2015, 11, 366
N and P co-doped mesoporous nanocarbon foams	0.5	55	735	Nat. Nanotechnol. 2015, 10, 444
Cu-Pt nanocage	2.0	-	560	ACS Catal. 2015, 5, 1445
Nanoporous carbon nanofiber films	2.0	185	626	Adv. Mater. 2016, 28, 3000
PAP-NCNCs	**0.5**	**96**	**728**	**This work**

Supplementary References

[S1] A. C. J. Heinrich, B. Thiedemann, P. J. Gates and A. Staubitz, *Org. Lett.*, 2013, **15**, 4666.

[S2] W. Stöber and A. E. Bohn, *J. Colloid Interface Sci.*, 1968, **26**, 62.

[S3] J. Zhang, Z. Zhao, Z. Xia and L. Dai, *Nat. Nanotechnol.*, 2015, **10**, 444.